Ultrafast Neuromorphic Dynamics Using Hidden Phases in the Prototype of Relaxor Ferroelectrics

Sergey Prosandeev,[1] Julie Grollier,[2] Diyar Talbayev,[3] Brahim Dkhil,[4] and L. Bellaiche[1]
[1]*Physics Department and Institute for Nanoscience and Engineering, University of Arkansas, Fayetteville, Arkansas 72701, USA*
[2]*Unité Mixte de Physique, CNRS, Thales, Université Paris-Saclay, 91767 Palaiseau, France*
[3]*Department of Physics and Engineering Physics, Tulane University, 6400 Freret Street, New Orleans, Louisiana 70118, USA*
[4]*Laboratoire Structures, Propriétés et Modélisation des Solides, CentraleSupelec, Université Paris-Saclay, CNRS-UMR8580, 91190 Gif-sur-Yvette, France*

(Received 11 August 2020; accepted 18 December 2020; published 12 January 2021)

Materials possessing multiple states are promising to emulate synaptic and neuronic behaviors. Their operation frequency, typically in or below the GHz range, however, limits the speed of neuromorphic computing. Ultrafast THz electric field excitation has been employed to induce nonequilibrium states of matter, called hidden phases in oxides. One may wonder if there are systems for which THz pulses can generate neuronic and synaptic behavior, via the creation of hidden phases. Using atomistic simulations, we discover that relaxor ferroelectrics can emulate all the key neuronic and memristive synaptic features. Their occurrence originates from the activation of many hidden phases of polarization order, resulting from the response of nanoregions to THz pulses. Such phases further possess different dielectric constants, which is also promising for memcapacitor devices.

DOI: 10.1103/PhysRevLett.126.027602

Neuromorphic computing combines physical artificial neurons and synapses to decrease the energy cost and speed up the inference and learning process of artificial intelligence. Biological neurons integrate the input spikes that they receive from other neurons. When their membrane exceeds a potential threshold, it undergoes a transient change of its electric charge, called action potential, which is then transmitted to other neurons through synapses. Synapses are at the heart of learning in biological and artificial neural networks. The strength with which they connect neurons is changed according to the activity of neurons. In artificial neural networks they are represented by a real value weight that should be memorized and evolves in a cumulative way during learning.

Three major features are typically looked for in materials used to emulate neurons and synapses. The first one is the ability of the material to emit action potentials just like biological neurons. The second one is the capacity of the material to integrate such input spikes in order to emulate the integration process in neurons and the cumulative changes of synapses weights. The third is the capacity of the material to exhibit multiple, nonvolatile states for emulating synaptic weights.

Memristive materials are today thoroughly investigated because they display these three properties [1–4]. Through different physical effects including filamentary switching, phase changes, and magnetization or polarization changes, they exhibit multiple conductance states that can be finely controlled through the application of pulses of electric fields or voltage. Memristors with a short term memory, also called volatile memristors, mimic neurons [5], whereas memristors with a long term, nonvolatile memory, can emulate synapses [6]. So far, the typical frequencies of memristive materials, such as resistive switching, phase change, spintronics, and ferroelectric technologies, is below the GHz [1,4,7,8]. Having THz as characteristic frequencies for neuromorphic computing would allow highly desired ultrafast processing of data and lower energy consumption [9–14].

Another currently active and exciting research field explores the generation of new "hidden" metastable states of matter by ultrafast optical excitation. Such states are referred to as hidden because they are not accessible via the tuning of thermodynamic variables, such as temperature or pressure. Optically induced ultrafast transitions to hidden states have been found in superconductors [15], colossal magnetoresistance manganites [16], charge-density wave materials [17], and incipient ferroelectrics [18,19]. A variety of optical excitation wavelengths have been used to trigger the transition to the hidden phase, ranging from visible [17] to midinfrared [15,16] to THz wavelengths [18,20]. In an example most relevant to the present Letter, ferroelectricity was induced in the quantum paraelectric $SrTiO_3$ by a THz optical pulse [18]. These hidden metastable states often enable physical functionalities that do not exist in the equilibrium thermodynamic phase, such as novel electronic memory concepts [21].

Based on the fundamental and technological importance of the aforementioned fascinating features, one may wonder if there is a "wunderbar" type of materials that can

possess hidden ferroelectric states when subjected to different forms of electric pulses of THz frequencies; and exhibit the three key properties of neuromorphic materials: (i) action potentials, (ii) integration, and (iii) multiple tunable nonvolatile states. Can such systems also display (iv) different values of the dielectric constant when occupying these hypothetical different states? If so, a dramatic breakthrough can happen in the field of memcapacitors [22,23], for which the capacitance (instead of the resistance in memristors) experiences multiple internal nonvolatile states depending on the history of the excitation. Memcapacitors are thus promising towards applications taking advantage of low dissipative power.

The aim of this Letter is to demonstrate, via the use of atomistic approaches, that the prototype of relaxor ferroelectrics does satisfy all items (i)–(iv). This prototype is $Pb(Mg_{1/3}Nb_{2/3})O_3$ (PMN), which exhibits unusual properties at equilibrium. Examples include a Burns temperature, $T_d = 620$ K, below which the temperature behavior of the optical refraction index deviates from a linear dependence without emergence of birefringence [24]; another temperature, $T^\star = 400$ K, at which the dielectric permittivity has a maximum, but without any macroscopic polarization occurring down to 0 K [25]; and a freezing temperature, $T_f = 220$ K, below which polar nanoregions (that are finite-size polarized islands of matter in the subnanoscale range) acquire a static, frozenlike character [26]. As we are going to see, the response of such polar nanoregions to different forms of THz pulses is the key behind the realization of items (i)–(iv). Note also that two other studies [27,28] show multiple polarization states found in multilayered heterostructures based on ferroelectric $Pb(Zr_{0.2}Ti_{0.8})O_3$, but, here our present work points out multiple polarization states appearing (i) in a single material, PMN, rather than a heterostructure, and (ii) via the use of THz-frequency fields to manipulate the polarization.

Here, we employ the effective Hamiltonian approach developed for PMN in Refs. [29,30] but within a molecular dynamics (rather than a Monte Carlo) algorithm [31], in order to investigate time-dependent phenomena. In particular, we apply, along the pseudocubic [111] direction, electric pulses of the form

$$\mathbf{E}_p(t) = \mathbf{E}_0 \exp\left[-\frac{(t-t_0)^2}{\Delta^2}\right] \cos\left[\omega(t-t_0)\right], \qquad (1)$$

where E_0 is the magnitude of the pulse, t_0 is the position of the main maximum, ω is the angular frequency, Δ is the width of the Gaussian, and t is the time variable. Such pulse is therefore a product of a Gaussian and a cosine function, and mimics well experimentally recorded THz pulses [32,33]. Details about the effective Hamiltonian are provided in Supplemental Material [34].

Let us start by demonstrating the capacity of the material to emit action potentials. We apply at 10 K a single pulse of the form given by Eq. (1) and for which the parameters are as follows: $E_0 = 4\sqrt{3} \times 10^7$ V/m, $\Delta = 0.2$ ps, and $\nu = \omega/2\pi = 1.5$ THz (note that our computational electric fields are typically about 22 times larger than measured ones in PMN [35], which is typical for atomistic effective Hamiltonian simulations [36]). Figure 1(a) shows an example of such a pulse, and also provides the time evolution of the polarization. The initial state is a relaxor state whose local dipole pattern is displayed in Fig. 1(b) and that possesses polar nanoregions (PNRs) inside which dipoles are nearly parallel to each other (note that we numerically found such PNRs, which are delimited in red in Figs. 1(b)–1(d), by applying a Bayesian algorithm to an instantaneous snapshots as in Ref. [37]). Consequently, its polarization is vanishing as a result of the fact that different polar nanoregions exhibit different directions for their local dipoles (note that the overall polarization is not exactly zero here because of finite-size effects associated with the used supercell). The activation of the single pulse then allows the system to possess an electrical polarization along the [111] direction that is increasing up to a value of 0.15 C/m^2 at 1.5 ps, while the maximum of the electric field pulse happens at 1 ps. Such a fact indicates a time delay between the applied pulse and the polarization response of the

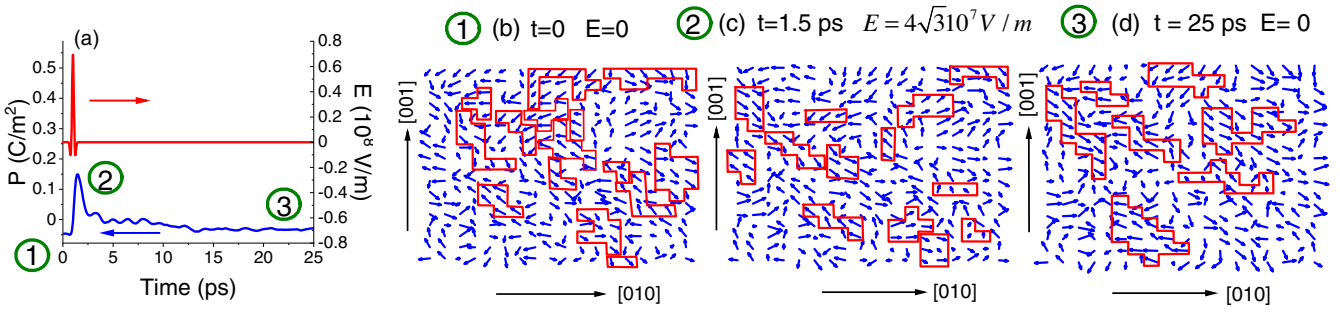

FIG. 1. Temporal evolution of the electrical polarization (a) and corresponding snapshots of the dipole patterns (b)–(d) in PMN at 10 K subject to a single pulse of the electric field (shown in panel (a) with the parameters $E_0 = 4\sqrt{3} \times 10^7$ V/m, $\Delta = 0.2$ ps, and $\nu = \omega/2\pi = 1.5$ THz in Eq. (1). The arrows in panels (b)–(d) show the local electric dipoles and the red lines delimit polar nanoregions at these snapshots.

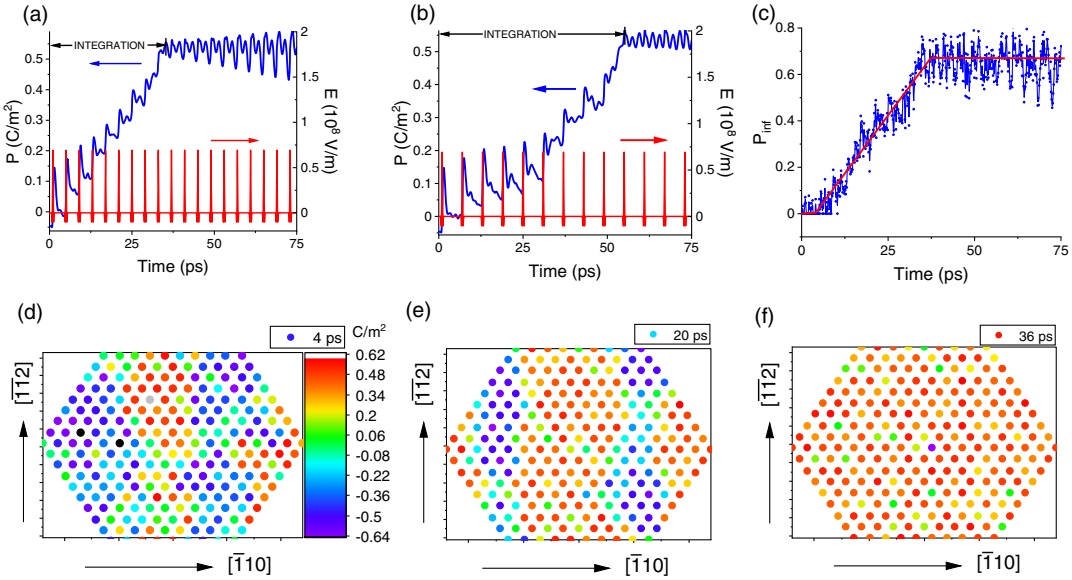

FIG. 2. (a) Temporal evolution of the polarization subject to a train of pulses separated by 4 ps [the other parameters of the pulses are the same as in Fig. 1(a)]; (b) the same as (a), but with a separation of the pulses by 6 ps; (c) Percolation strength as a function of time, for the train of pulses corresponding to panel (a); (d)–(f) z component of the polarization subject to the train of pulses shown in panel (a) at different times (note that the z axis is along the [111] pseudocubic direction).

system, which is reminiscent of the time delay of the polarization found in other inhomogeneous systems when under external stimulus [38]. The dipolar pattern associated with this maximal polarization of 0.15 C/m^2 is displayed in Fig. 1(c), and, in comparison with Fig. 1(a), demonstrates that the emergence of this sizable polarization basically originates from electric dipoles elongating along (or rotating towards) the [111] field direction. Then, after the pulse has been switched off, the system gradually moves back towards another relaxor state, also having a nearly vanishing polarization and polar nanoregions. Strikingly, the activation of a new state from an original state by a physical stimulus and then its return to a state having similar macroscopic properties precisely characterizes a neuron behavior when it is excited and emits an action potential [39]. In other words, Fig. 1(a) represents an original way to mimic in materials, at the THz range the spiking of a neuron, which in biology occurs at hundreds of Hz, while Figs. 1(b)–1(d) reveal the microscopic pictures associated with such function.

We now study if the relaxor can mimic the second important feature of synaptic and neuronic materials, which is the ability to integrate incoming spikes. For this purpose, we apply trains of THz pulses to the relaxor with different intervals in between the pulses. Figures 2(a) and 2(b) show the pulse train with an interspike interval of, respectively, 4 and 6 ps, along with its effect on polarization. The polarization experiences an increase after every pulse along the [111] direction and does not come back to its nearly vanishing initial value. This gradual enhancement of polarization that occurs faster when spikes are more often applied, demonstrates the integration property of the relaxor material.

For times larger than 35 ps in Fig. 2(a) and 52 ps in Fig. 2(b), the system then oscillates around a ferroelectric state having a rather large polarization of $\simeq 0.5$ C/m^2 when the train of pulses continues to be applied. In other words, the application of such a train of pulses has allowed the stabilization of a ferroelectric state having a nonzero net polarization from a relaxor state with a zero net polarization, while a *single* pulse of the same magnitude, width, and frequency resulted in the return to a relaxor state after a certain time [as indicated in Fig. 1(a)]. The stabilization of such a ferroelectric state is therefore symptomatic of the creation of a so-called hidden phase that is metastable in nature, as similar to the THz activation of a ferroelectric state from a quantum paraelectric phase in $SrTiO_3$ [18].

In order to reveal and understand the unusual behavior of the polarization depicted in Fig. 2(a), we display in Figs. 2(d)–2(f) the corresponding evolution of the dipolar structure in a given plane and at different times, as well as compute and report in Fig. 2(c) the so-called infinite percolation cluster strength, which is three dimensional in nature and that is defined as [40]

$$P_{\mathrm{inf}} = \frac{n_{\mathrm{inf}}}{N}, \tag{2}$$

where N is the total number of Pb sites in the supercell and n_{inf} is the number of Pb sites belonging to the infinite percolation cluster, that is the cluster that spreads over the whole supercell, from one boundary to the opposite one.

Figures 2(c) and 2(d) basically show that at ≃4 ps (after the first pulse has been applied and died out), the dipolar structure consists of that of a relaxor state, for which the strength of the infinite percolation cluster is zero. However, after that and up to ≃35 ps in Fig. 2(a), the local dipoles have the tendency to gradually turn their direction towards that of the field applied along [111], while P_{inf} linearly increases with time in overall, which is characteristic of a gradual merging and percolation of some polar nanoregions. The various peaks and dips of P_{inf} are associated with the different pulses of electric fields and indicate that the infinite percolation cluster breathes "out" and "in" with the application and passing of the pulses, respectively. Then, for times above ≃35 ps in Fig. 2(a), the states oscillate with the pulses around a ferroelectric state consisting of many dipoles, but not all, having a significant component along [111], along with the infinite percolation cluster having a significant strength of about 0.67.

The effects of the parameters associated with a train of electric pulses [that are, E_0, Δ, ω of Eq. (1) and the shape of the electric field pulse], on their integration through of the time evolution of the polarization are shown and discussed in the Supplemental Material [34]. For both neurons and synapses, it is important to be able to bring back the polarization to lower values once the system has reached saturation. Figure S7 [34] shows that the system can be reset to its initial relaxor state with vanishing polarization by heating it up to room temperature, above the so-called depolarizing temperature—which is of about 220 K in PMN [25], and then cooling it back to 10 K. Figure S8 [34] shows that the system can also be gradually brought back to polarization values between $+\simeq 0.5$ and $\simeq -0.5$ C/m^2 by applying the same train of pulses as in Fig. 2(a), but with opposite direction of the electric field and a larger amplitude of that field.

We now investigate if multiple polarization states can be reached and stabilized in PMN depending on the history of the applied electric fields, which is key to emulate synapses and achieve learning [4,9,10]. To address such question, we conducted eight different simulations that distinguish themselves by the time at which pulses of electric fields are stopped to be applied, that are 4, 8, 12, 16, 20, 24, 28, and 32 ps [note that all the other parameters of these trains of pulses are those of Fig. 2(a)]. The results of these eight simulations are indicated in Fig. 3.

For the first and second chosen times, one can see that the system comes back to a relaxor state, which is characterized by a vanishing overall polarization. On the other hand, from the third to seventh times, after pulses are not applied anymore, the system evolves and maintains different ferroelectric states of increasing polarization. This ability to obtain multiple polarization values or weights corresponds to the spiking-dependent plasticity used in synapses for learning. These different states can also be considered as other hidden phases in PMN that we explored thanks to various THz spiking rates. Finally, for the largest time of 32 ps, PMN then first continues to increases its polarization and then relaxes towards the ferroelectric state with a maximum polarization of over 0.55 C/m^2. The results of Fig. 3 are thus promising towards neuromorphic applications taking advantage of such ultrafast solid-state synaptic memristors. Note that Fig. S9 of Ref. [34] indicates how the change of the chosen initial relaxor state can influence the number and time stability of hidden states.

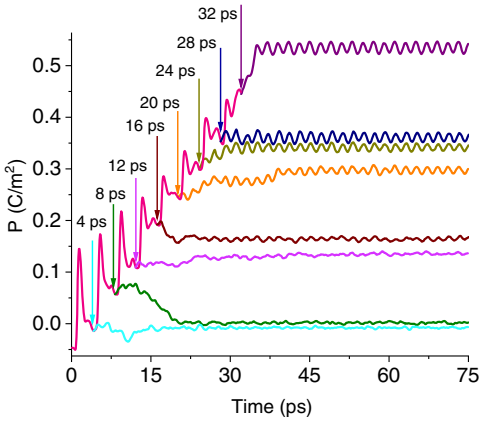

FIG. 3. Multiple nonvolatile polarization states (in magenta color) found at different times for the case of the train of the electric field pulses shown in Fig. 2(a). The lines shown with the other colors were found under no-field condition, after turning off the field at the times marked by arrows of the same color in this figure.

We also calculated the dielectric susceptibility (more precisely, one-third of the trace of the dielectric tensor) in these intermediate states, by using a cumulant method [41] within a Monte Carlo effective Hamiltonian scheme. We obtained a large variation and multiple values of such physical quantity at 10 K: namely, 2216, 472, 477, 434, 367, 388, 400, and 219, for all the intermediate states found in Fig. 3, to be compared with 546 and 232 for the initial relaxor state and the fully polarized ferroelectric phase, respectively. The large value for the first intermediate state likely originates from it being at the border of adopting an electrical polarization. Such large variation can be put in use to the design of *memcapacitors*.

We also computed the strength of the infinite percolation clusters in each of these eight cases after the pulses have been turned off and the system has relaxed to its equilibrium states. We found that P_{inf} of the relaxed states is basically linked to the polarization of these relaxed states via the red curve of Fig. 2(c), implying that it increases with the value of the time at which pulses of electric fields are turned off in our eight simulations. Interestingly, Fig. 3 shows that each of these relaxed states continues to oscillate even after the pulses have been long turned off. Such oscillations are associated with a frequency of about 0.5 THz, or, equivalently, 17 cm^{-1}, which is about the low frequency of vibrational modes observed by several

groups (see Ref. [42] and references therein, with such agreement being a further proof that our simulations are accurate).

In summary, we report that PMN can have a multitude of hidden phases with controllable magnitude of electrical polarization and dielectric response, as well as neuronic behavior, when subject to different THz pulses of electric field or voltage below the freezing temperature—which corresponds to the ability of the system to explore many out-of-equilibrium states in the quasiflat energy landscape characteristic of these complex materials. The origin of these features resides in the ultrafast readaptation of polar nanoregions to THz excitation, as consistent with the low-frequency of vibrational modes (about 0.5 and 2.4 THz) known to occur in PMN below the freezing temperature [43]. Since polar nanoregions and nonlinear response exist in other relaxor ferroelectrics, including room-temperature and lead-free ones [44], we hope that our results open a new field of research dedicated to employ this special class of materials, as well as others possessing hidden phases, for the design of new THz functionalities (including memcapacitors) but also of ultrafast neuromorphic architecture and computing.

This work was supported by ONR Grant No. N00014-17-1-2818 and the Vannevar Bush Faculty Fellowship (VBFF) from the Department of Defense. J. G. acknowledges support from Q-MEEN-C, an Energy Frontier Research Center funded by the U.S. Department of Energy (DOE), Office of Science, Basic Energy Sciences (BES), under Award No. DE-SC0019273, for work on neuromorphic computing with relaxors. D. T. acknowledges support from NSF for work on terahertz-driven ferroelectric dynamics under Grant No. DMR-1554866.

[1] V. Milo, G. Malavena, C. M. Compagnoni, and D. Ielmini, J. Mater. **13**, 166 (2020).
[2] Y. Wang, H. Wu, G. W. Burr, C. S. Hwang, K. L. Wang, Q. Xia, and J. J. Yang, Nat. Rev. Mater. **5**, 173 (2020).
[3] D. Monroe, Commun. ACM **57**, 13 (2014).
[4] S. Boyn, J. Grollier, G. Lecerf, B. Xu, N. Locatelli, S. Fusil, S. Girod, C. Carrétéro, K. Garcia, S. X. J. Tomas, L. Bellaiche, M. Bibes, A. Barthélémy, S. Saighi, and V. Garcia, Nat. Commun. **8**, 14736 (2017).
[5] M. D. Pickett, G. Medeiros-Ribeiro, and R. S. Williams, Nat. Mater. **12**, 114 (2013).
[6] S. H. Jo, T. Chang, I. Ebong, B. B. Bhadviya, P. Mazumder, and W. Lu, Nano Lett. **10**, 1297 (2010).
[7] M. Romera, P. Talatchian, S. Tsunegi, F. A. Araujo, V. Cros, P. Bortolotti, J. Trastoy, K. Yakushiji, A. Fukushima, H. Kubota, S. Yuasa, M. Ernoult, D. Vodenicarevic, T. Hirtzlin, N. Locatelli, D. Querlioz, and J. Grollier, Nature (London) **563**, 230 (2018).
[8] J. Torrejon, M. Riou, F. A. Araujo, S. Tsunegi, G. Khalsa, D. Querlioz, P. Bortolotti, V. Cros, K. Yakushiji, A. Fukushima, H. Kubota, S. Yuasa, M. D. Stiles, and J. Grollier, Nature (London) **547**, 428 (2017).
[9] J. Grollier, D. Querlioz, K. Y. Camsari, K. Everschor-Sitte, S. Fukami, and M. D. Stiles, Nat. Electron., https://doi.org/10.1038/s41928-019-0360-9 (2020).
[10] D. Markovic, A. Mizrahi, D. Querlioz, and J. Grollier, J. Phys. Neuromorphic Comput. arXiv:2003.04711.
[11] R. Khymyn, I. Lisenkov, J. Voorheis, O. Sulymenko, O. Prokopenko, V. Tiberkevich, J. Akerman, and A. Slavin, Sci. Rep. **8**, 15727 (2018).
[12] A. Chakravarty, J. H. Mentinka, C. S. Davies, K. T. Yamada, A. V. Kimel, and Th. Rasinga, Appl. Phys. Lett. **114**, 192407 (2019).
[13] J. Feldmann, N. Youngblood, M. Karpov, H. Gehring, and X. Li, arXiv:2002.00281.
[14] M. L. Schneider, C. A. Donnelly, I. W. Haygood, A. Wynn, S. E. Russek, M. A. Castellanos-Beltran, P. D. Dresselhaus, P. F. Hopkins, M. R. Pufall, and W. H. Rippard, Sci. Rep. **10**, 934 (2020).
[15] D. Fausti, R. I. Tobey, N. Dean, S. Kaiser, A. Dienst, M. C. Hoffmann, S. Pyon, T. Takayama, H. Takagi, and A. Cavalleri, Science **331**, 189 (2011).
[16] M. Rini, R. Tobey, N. Dean, J. Itatani, Y. Tomioka, Y. Tokura, R. W. Schoenlein, and A. Cavalleri, Nature (London) **449**, 72 (2007).
[17] L. Stojchevska, I. Vaskivskyi, T. Mertelj, P. Kusar, D. Svetin, S. Brazovskii, and D. Mihailovic, Science **344**, 177 (2014).
[18] X. Li, T. Qiu, J. Zhang, E. Baldini, J. Lu, A. M. Rappe, and K. A. Nelson, Science **364**, 1079 (2019).
[19] T. F. Nova, A. S. Disa, M. Fechner, and A. Cavalleri, Science **364**, 1075 (2019).
[20] M. Liu, H. W. Hwang, H. Tao, A. C. Strikwerda, K. Fan, G. R. Keiser, A. J. Sternbach, K. G. West, S. Kittiwatanakul, J. Lu, S. A. Wolf, F. G. Omenetto, X. Zhang, K. A. Nelson, and R. D. Averitt, Nature (London) **487**, 345 (2012).
[21] I. Vaskivskyi, I. A. Mihailovic, S. Brazovskii, J. Gospodaric, T. Mertelj, D. Svetin, P. Sutar, and D. Mihailovic, Nat. Commun. **7**, 11442 (2016).
[22] Z. Wang, M. Rao, J. Han, J. Zhang, P. Lin, Y. Li, C. Li, W. Song, S. Asapu, R. Midya, Y. Zhuo, H. Jiang, J. H. Yoon, N. K. Upadhyay, S. Joshi, M. Hu, J. P. Strachan, M. Barnell, Q. Wu, H. Wu, Q. Qiu, R. S. Williams, Q. Xia, and J. J. Yang, Nat. Commun. **9**, 3208 (2018).
[23] J. Martinez-Rincon, M. Di Ventra, and Yu. V. Pershin, Phys. Rev. B **81**, 195430 (2010).
[24] G. Burns and F. H. Dacol, Phys. Rev. B **28**, 2527 (1983).
[25] B. Dkhil, P. Gemeiner, A. Al-Barakaty, L. Bellaiche, E. Dulkin, E. Mojaev, and M. Roth, Phys. Rev. B **80**, 064103 (2009).
[26] E. V. Colla, E. Yu. Koroleva, N. M. Okuneva, and S. B. Vakhrushev, Phys. Rev. Lett. **74**, 1681 (1995).
[27] G. A. Boni, L. D. Filip, C. Chirila, I. Pasuk, R. Negrea, I. Pintilie, and L. Pintilie, Nanoscale **9**, 19271 (2017).
[28] G. A. Boni, L. D. Filip, C. Chirila, A. Iuga, I. Pasuk, L. Hrib, L. Trupina, I. Pintilie, and L. Pintilie, Phys. Rev. Applied **12**, 024053 (2019).
[29] A. Al-Barakaty, S. Prosandeev, D. Wang, B. Dkhil, and L. Bellaiche, Phys. Rev. B **91**, 214117 (2015).

[30] S. Prosandeev, S. Prokhorenko, Y. Nahas, A. Al-Barakaty, L. Bellaiche, P. Gemeiner, D. Wang, A. A. Bokov, Z.-G. Ye, and B. Dkhil, Phys. Rev. B **102**, 104110 (2020).
[31] D. Wang, J. Hlinka, A. A. Bokov, Z.-G. Ye, P. Ondrejkovic, J. Petzelt, and L. Bellaiche, Nat. Commun. **5**, 5100 (2014).
[32] H. Hirori, A. Doi, F. Blanchard, and K. Tanaka, Appl. Phys. Lett. **98**, 091106 (2011).
[33] S. Lin, S. Yu, and D. Talbayev, Phys. Rev. Applied **10**, 044007 (2018).
[34] See Supplemental Material at http://link.aps.org/supplemental/10.1103/PhysRevLett.126.027602 for more details. Firstly, to investigate the effect of different parameters associated with a pulse train and of the temperature with respect to the results depicted in Fig. 2(a) of the main text. Secondly, we demonstrate how to "reset" the system.
[35] Z. Jiang, Y. Nahas, S. Prokhorenko, S. Prosandeev, D. Wang, J. Îñiguez, and L. Bellaiche, Phys. Rev. B **97**, 104110 (2018).
[36] B. Xu, J. Iniguez, and L. Bellaiche, Nat. Commun. **8**, 15682 (2017).
[37] S. Prosandeev, D. Wang, and L. Bellaiche, Phys. Rev. Lett. **111**, 247602 (2013).
[38] I. Ponomareva and L. Bellaiche, Phys. Rev. Lett. **101**, 197602 (2008).
[39] Z. Wang *et al.*, Nat. Electron. Rev. **1**, 137 (2018).
[40] D. Stauffer and A. Aharony, *Introduction to Percolation Theory* (Taylor & Francis, London, 1994).
[41] K. M. Rabe and E. Cockayne, in *5th Williamsburg Workshop*, edited by R. E. Cohen (AIP, New York, 1988), p. 61.
[42] B. Hehlen, M. Al-Sabbagh, A. Al-Zein, and J. Hlinka, Phys. Rev. Lett. **117**, 155501 (2016).
[43] S. B. Vakhrushev and S. M. Shapiro, Phys. Rev. B **66**, 214101 (2002).
[44] A. R. Akbarzadeh, S. Prosandeev, E. J. Walter, A. Al-Barakaty, and L. Bellaiche, Phys. Rev. Lett. **108**, 257601 (2012).